JOURNAL OF PROPULSION AND POWER
Vol. 27, No. 4, July–August 2011

Hall-Effect Thruster–Cathode Coupling, Part I: Efficiency Improvements from an Extended Outer Pole

Jason D. Sommerville* and Lyon B. King†
Michigan Technological University, Houghton, Michigan 49931

DOI: 10.2514/1.50123

This is the first part of a two-part paper in which the effect of cathode position and magnetic field configuration on Hall-effect thruster performance is explored. In this part, the effect of the cathode position on the efficiency of the thruster is explored. The study consists of two experiments performed on a Hall-effect thruster with its outer pole modified so as to change the external magnetic field topology with respect to the cathode position. In these experiments, the efficiency of the modified thruster is compared with the efficiency of the Hall-effect thruster in its original configuration. The importance of the magnetic field separatrix, a surface which divides the magnetic field lines into internal and external regions, is shown. The modifications provide a means to improve cathode coupling while keeping the cathode outside of the ion beam, which can erode the cathode components. The improvement in cathode coupling results in improved thruster performance, specifically improved cathode coupling voltages (the potential between the cathode and facility ground) of approximately 3% of the discharge voltage, increased beam divergence efficiencies on the order of 5 percentage points, and an improvement in total efficiency of up to 10 percentage points are noted.

Nomenclature

I_d	=	anode supply current
$\dot{m}$	=	mass flow rate
$\dot{m}_a$	=	anode mass flow rate
$\dot{m}_c$	=	cathode mass flow rate
r	=	radial position relative to the thruster axis; negative values indicate positions opposite the thruster axis from the cathode
T	=	thrust
V_{cg}	=	cathode coupling voltage
V_d	=	anode supply voltage
z	=	axial position downstream from the exit plane of the thruster
η	=	thruster efficiency
η_a	=	anode efficiency
η_t	=	total efficiency
η_{Vcg}	=	cathode coupling efficiency

I. Introduction

HALL-EFFECT thrusters (HETs) are a class of electric propulsion device that use electric and magnetic fields to create a plasma and expel the ions at high velocity to generate thrust [1]. A critical component of the HET is the cathode. The cathode is a plasma source that provides free electrons that serve two purposes. The first purpose is beam neutralization: sufficient electrons are expelled via the cathode to balance the charge emitted by the ion beam. The second purpose is to provide the "seed" electrons which initialize and sustain the plasma discharge near the exit plane of the HET. The flow of the seed electrons is known as the recycle current.

Presented as Paper 2009-5004 at the 45th AIAA/ASME/SAE/ASEE Joint Propulsion Conference & Exhibit, Denver Colorado, 2–5 August 2009; received 31 March 2010; revision received 19 January 2011; accepted for publication 1 February 2011.

*Currently Chief Technologist, Aerophysics, Inc., 1402 E. Sharon Ave., Ste. 206. Student Member AIAA.

†Associate Professor, Dept. of Mechanical Engineering, Engineering Mechanics, 815 R. L. Smith Bldg., 1400 Townsend Dr. Member AIAA.

Because collisions and magnetic fields impede the motion of the electrons toward the ion beam and anode, work is required simply to get the electrons to where they are needed for the plasma to maintain quasi neutrality. This work is an efficiency loss mechanism, as it does not directly generate thrust. The cathode coupling voltage (V_{cg}) provides a rough measure of the amount of work required to move the electrons from the cathode. In the laboratory, this is the potential at which the cathode floats below ground. In space with negligible electric fields compared with that generated by the thruster, the ambient plasma potential serves the same function as ground. In this work, V_{cg} is negative by convention.

To understand why V_{cg} is the correct measure of the coupling efficiency, consider an ion "falling" out of the thruster. While most of the potential drop occurs inside the thruster, there is some small drop all they way through the sheath at the tank wall at the end of the ion's trajectory. The ion is accelerated through this drop, and the opposite force pushes back on the thruster, generating the thrust. When the ion reaches the tank wall, it impacts the surface, combines with an electron from the surface, and exits the system as a neutral. To maintain charge neutrality, an electron from the cathode must also travel to the tank wall to make up for the electron that neutralized the ion. The anode is biased at V_d volts with respect to the cathode. Assuming no efficiency loss mechanisms affect the ionization and acceleration of the ions, a singly ionized ion should hit the tank wall with $E_d = eV_d$ of energy *unless* it also requires some energy to move the electron from the cathode to the wall. If we denote this energy by E_{cg} then the energy that the ion receives can be no more than $E_d - E_{\text{cg}}$, which implies that the ion starts at a potential of $V_d - V_{\text{cg}}$ where $V_{\text{cg}} = E_{\text{cg}}/e$. Furthermore, since it requires E_{cg} of energy to move the electron to the wall, the cathode must be at a potential V_{cg} relative to the tank wall.

Figure 1 illustrates this efficiency cost. In Case A, the cathode floats lower than in Case B, that is, $V_{\text{cg}}A < V_{\text{cg}}B$. The maximum potential drop available to an ion is $V_{\text{acc}} = V_d - V_{\text{cg}}$. Obviously, Case B with the higher V_{cg} has a higher V_{acc} and therefore more energy is available to the ions. Therefore, all other things being equal, the efficiency of Case B will be higher than that of Case A.

A few researchers have studied the effects of cathode type [2] and mass flow rate [2,3] on HET performance. Albaréde et al. [2] compared three types of thermionic orificed cathodes and found only small differences in behavior. Both Albaréde et al. and Tilley et al. [3] observed increases in cathode coupling voltage with increasing flow rate, and Albaréde et al. [2] also noticed correlated, nonmonotonic changes in anode current fluctuation frequency with changes in

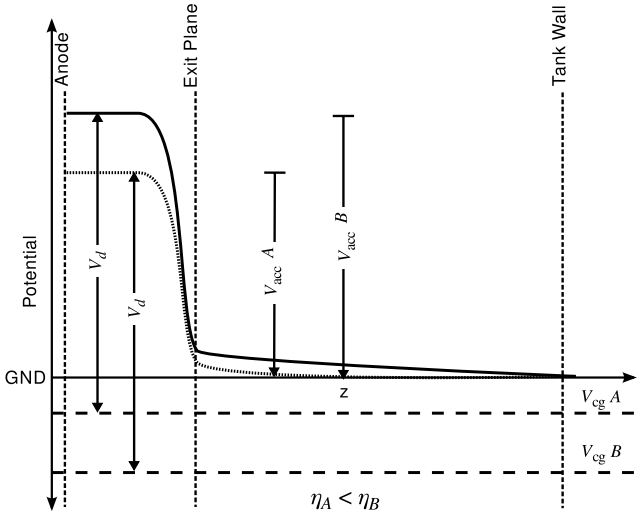

Fig. 1 The effect of cathode coupling voltage on energy available for ion acceleration.

cathode mass flow rate [2]. It has been repeatedly noted that cathode placement has an effect on thruster performance [3–8]. Hofer and Gallimore [4] and Jameson et al. [8] noticed significant performance improvements by placing the cathode in the center of the HET such that the cathode axis coincides with the thruster axis rather than placing it external to the body of the thruster, and Beal et al. [6] have inferred from probe measurements that cathode placement and number in a cluster of HETs will affect the total efficiency of the thruster. There are two studies available in the literature that specifically address the effect of cathode position on thruster performance across a range of cathode locations. In the first, by Tilley et al. [3], the authors note an increase in cathode coupling voltage as the cathode is moved downstream of the exit plane. In the second, by Walker and Gallimore [7], the authors note decreasing performance as the cathode is moved radially away from the thruster. This is in contradiction to some of our own work in which we see generally improved performance with increasing cathode separation for cathodes mounted outside of the thruster body [9,10]. The discrepancy may be due to the difference in thruster size, magnetic field configurations, and the difference in overall range of cathode positions over which the two experiments were performed.

This paper focuses on the effect of the magnetic field separatrix. The separatrix is a line or surface which divides the magnetic field into independent regions of similarly connected flux lines. Separatrices are flux lines which pass through magnetic null points (also known as stagnation points) [11]. Any dipole source, such as a magnet coil, will exhibit a separatrix along its axis The addition of each dipole to an HET which adds a (nondegenerate) magnetic null point adds new separatrices. Thus, thrusters will exhibit separatrices in proportion to their topological similarity to higher order multipoles.

Figure 2a shows an axisymmetric HET, which acts behaves as a linear quadropole. The white inner and middle coils carry current out of the page, as denoted by dots, and the white outer coil carries current into the page, as denoted by *x*s. Current need be on only one of the inner and middle coils for a similar field to be generated. The source distribution is topologically identical to the quadropole formed by rings of opposing current, the cross section of which is shown in Fig. 2b. Note that in both figures there are two separtricies, one along the *z*-axis, and a second surface which originates between the opposing current sources. The addition of the iron magnetic circuit only adjusts the location of the flux lines.

Any HET that is topologically similar will include this separatrix. This includes all HETs with magnetic coils centered off-axis, including the BPT-2000 used in these experiments. On these HETs, the separatrix divides the magnetic field into "internal" and "external" regions. Previous work suggested the importance of the magnetic field separatrix to cathode coupling processes [12]. The present research further establishes that placing the cathode within the separatrix leads to improved thruster performance.

On smaller thrusters, placing the cathode within the separatrix puts the cathode very close to the ion beam, as shown in Fig. 3. This position leads to increased cathode sputtering, thereby decreasing cathode lifetime. To overcome this problem, we have extended the outer pole of an Aerojet BPT-2000 [13] to reposition the separatrix further from the ion beam. Operation of the thruster at the same operating conditions, including cathode position, shows that the increased thruster efficiency can be achieved by using the extended outer pole and placing the cathode within the separatrix. In two experiments, we show the importance of the separatrix and the improvement achieved with the extended outer pole. In this paper we focus on the modifications made, their effect on the magnetic field, and the changes in the anode efficiency and cathode coupling voltage. In the accompanying paper [14], we discuss the ion beam and near-field plume properties associated with each of the configurations and relate these back to the thruster performance.

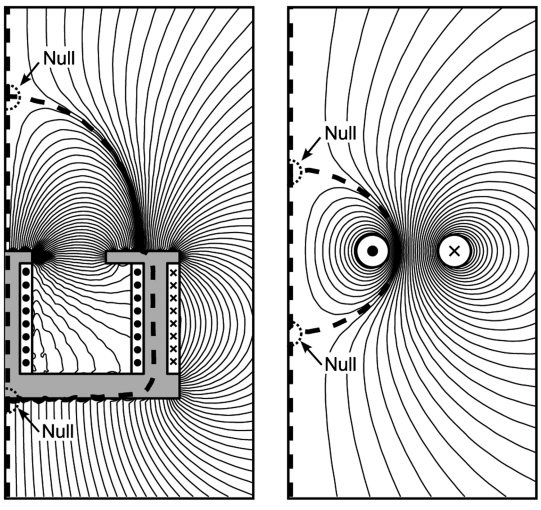

a) HET **b) Equivalent quadropole**

Fig. 2 The axisymmetric HET shown in part a is topologically equivalent to the quadropole formed by two rings of opposing current in part b.

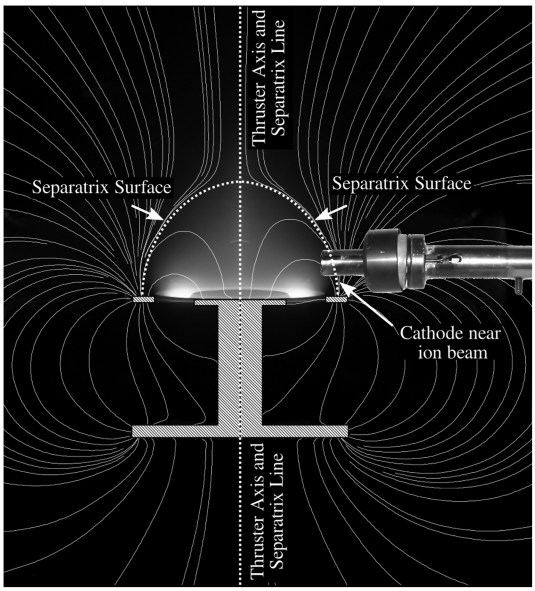

Fig. 3 The magnetic field separatrix of an HET. The solid lines are magnetic field lines. The dashed lines show the separtrices. Placing the cathode inside of the separatrix puts it dangerously close to the ion beam.

II. Experiments

A. Extended Outer Pole

By extending the size of the outer pole, the position of the separatrix was changed. Figures 4a and 4b show drawings of the pole pieces and photographs of the pieces mounted to the thruster. Figure 4c shows the calculated magnetic fields of each configuration on the cross section of the thruster which passes through both the thruster axis and the cathode axis. The calculations were performed using a 3-D model in a commercial field solver. Further details may be found in Sommerville's dissertation [15]. The thruster used in this work has no inner coil, and the outer coils are wired in series. Therefore, as long as the magnetic iron does saturate, which it did not for any of the coil currents used in these experiments, the magnetic field is linear with coil current. Figure 4c shows that the field of the thruster is modified such that the separatrix is "inflated," as shown in Fig. 4c. With the original outer pole (OOP), the separatrix intersects the point ($z = 30$ mm, $r = 60$ mm). (The axial coordinate of $z = 30$ mm is chosen because the cathode is positioned along this line in the experiments.) With the extended outer pole (EOP), the separatrix intersects the point ($z = 30$ mm, $r = 78$ mm), 18 mm radially farther than with the OOP.

B. Experiments Overview

To show the effect of the magnetic field separatrix we conducted two experiments. Experiment I is identical to a previous experiment [12] except that krypton was used as the propellant, and the outer pole type (original or extended) was an additional independent variable. Krypton was chosen because a global shortage of xenon at the time of these experiments made the use of xenon impractical. In two separate runs, one for each of the outer poles, the HET was mounted on a thrust stand. The mounting electrically connected the thruster to facility ground. The cathode was mounted on a linear motion stage so that its position could be moved from $r = 40$ mm to 250 mm radially away from the thrust axis at a fixed axial distance of $z = 30$ mm from the thruster exit plane (see Fig. 5). "Cathode position" refers to the position of the cathode orifice relative to the intersection of the

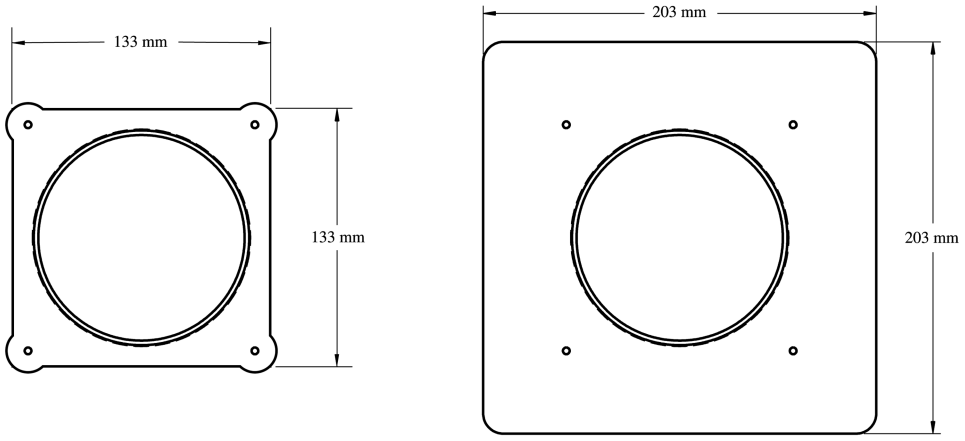

a) Drawings of the original and the extended outer pole pieces

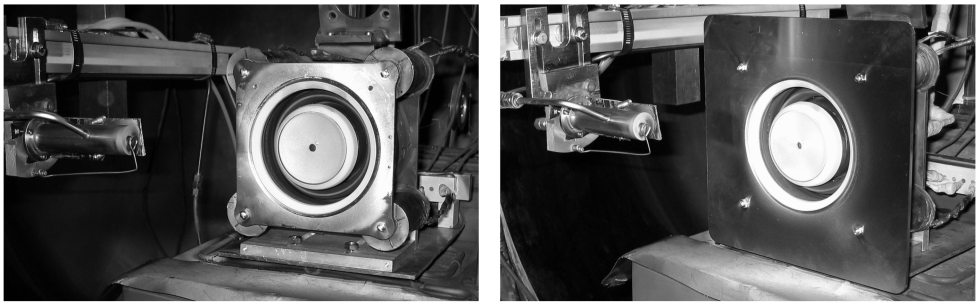

b) Photographs of the thruster with the original and the extended outer pole

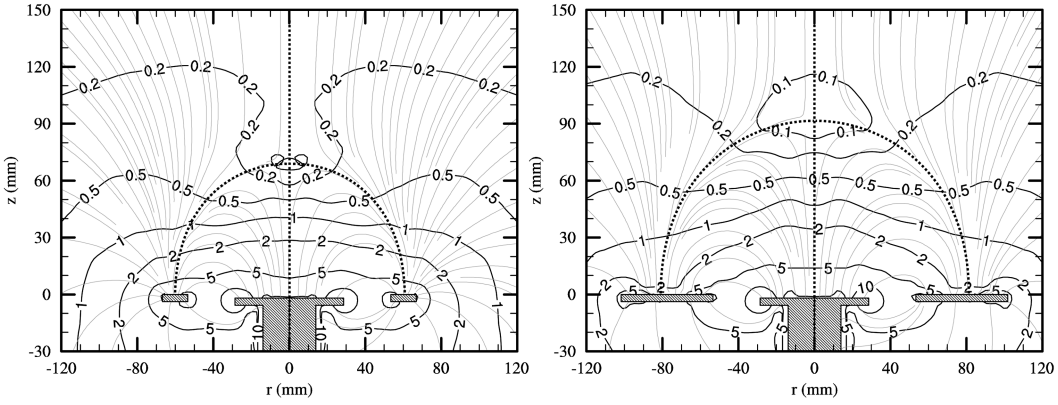

c) Magnetic field of the thruster with the original and the extended outer poles. The solid lines represent magnetic field lines, the labeled contour lines show magnetic field strength per magnet coil current in mT/A, the dotted lines show the position of the separatrices.

Fig. 4 Design and effect of the extended outer pole.

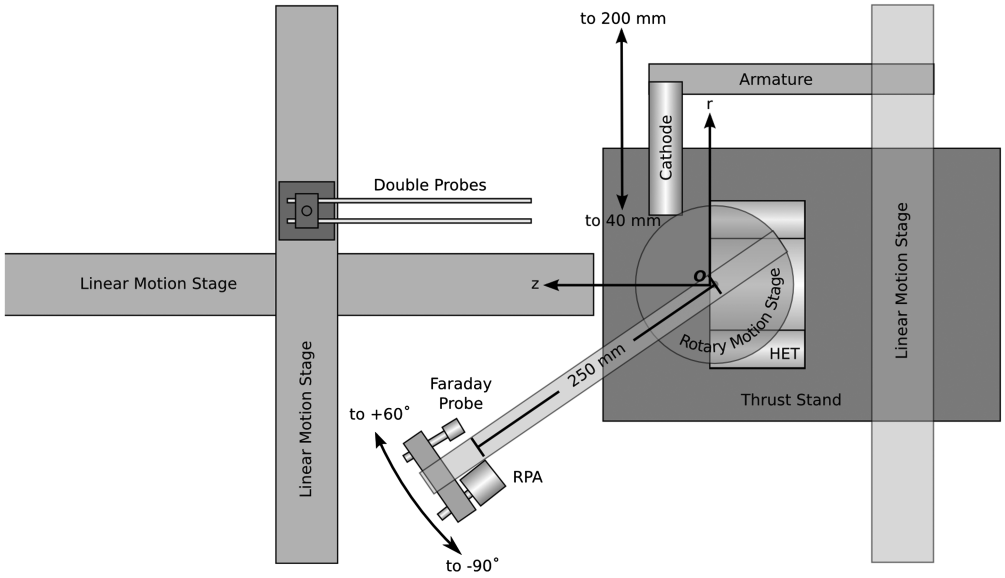

a) Schematic

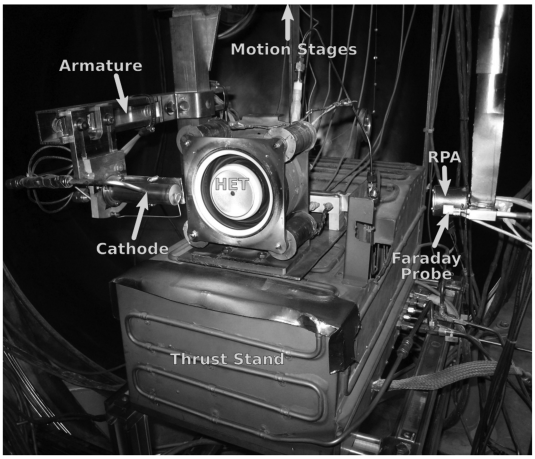

b) Photograph

Fig. 5 Experimental setup.

thruster axis and exit plane. The cathode was mounted with its axis at a 90 deg angle to the thrust axis to enable positioning of the cathode across a broad range of radial positions, including some in front of the face of the thruster. Cathode mass flow rates were varied between 2 and 10 SCCM. All other parameters were held constant. The experimental conditions are summarized in Table 1. A Faraday probe and a retarding potential analyzer (RPA) were placed on a boom mounted on a rotational stage directly above the intersection of the thrust axis and the exit plane. A double Langmuir probe was mounted on a two-axis motion table and used to measure the near-field plasma properties. The results of the probe data are used to understand the efficiency loss mechanisms of the thruster and are discussed in the companion paper [14].

Table 1 Experiment I conditions: parameters in *italics* were independent variables

Parameter	Value(s)	Units
Propellant	Krypton	
Anode voltage	250	V
Anode mass flow rate	2.553	mg/s
Cathode orientation	90	deg
Cathode axial z position	30	mm
Cathode radial r position	40, 50, 60, 70, 80, 90, 100, 120, 140, 180, 200, 250	mm
Cathode mass flow rate	0.125, 0.312, 0.623	mg/s
Outer pole	Original, extended	

Unfortunately, the thruster modified with the EOP would not maintain a discharge at the same magnet current as in the original experiment with the OOP over all of the cathode positions. Therefore, we conducted the portion of Experiment I that used the EOP at a lower magnetic field strength that maintained a discharge at all cathode positions.

To provide better direct comparison between the OOP and the EOP, we conducted Experiment II, in which the thruster was operated with both the OOP and the EOP with the cathode at a fixed location of ($z = 30$ mm, $r = 70$ mm). This location was chosen so that the cathode would be outside the separatrix with the OOP but inside of the separatrix with the EOP. In each case, the thruster was operated over a range of magnet currents, and the results compared.

C. Procedure

The thruster was configured with either the OOP or the EOP and mounted on the thrust stand. After evacuating the chamber the cathode was conditioned and the thruster started. The thruster was then operated until the system reached thermal equilibrium, as determined by watching the thrust and discharge current stabilize, typically about 30 min. At this point the thruster was extinguished, the thrust stand calibrated, and the thruster restarted.

In each experiment, the cathode was placed at a specific radial position and the cathode mass flow rate set. The thruster was set at an

operating voltage of 250 V and an anode mass flow rate of 2.553 mg/s of krypton. These values were chosen to match prior experiments conducted on cathode position with this thruster [9,10,12]. 2.553 mg/s of krypton is the volumetric flow rate equivalent of 4 mg/s of xenon. Equal volumetric flow rates were chosen in an attempt to minimize the changes in plume properties when changing from xenon to krypton. However because of the change in propellant, only comparisons to trends from the prior xenon experiments will be made. For the original outer pole, a magnet current value of 2.5 A was chosen, again, to match prior values. In the present experiments, 2.5 A was slightly above the optimal point as determined by the discharge current minimum, but more importance was placed on matching prior magnetic field strengths. With the extended outer pole, it was impossible to run the thruster at 2.5 A. Therefore, the optimal value of 1.5 A was chosen. All magnet current optimization was performed with the cathode located at $z = 100$ mm.

After the thruster stabilized, thrust, discharge current, and efficiency of the thruster were measured over a period of 90–120 s. After recording the performance, the cathode was moved to a new location, randomly chosen from the 14 radial positions: from 40 to 100 mm in 10 mm intervals, from 100 to 200 mm in 20 mm intervals, and 250 mm. The axial position remained fixed at $z = 30$ mm. After all of the performance data were taken at a given cathode mass flow rate the electrostatic probe data were acquired. The details of this are discussed in Part II [14].

After all performance and probe data were acquired at each of the cathode positions, the cathode mass flow rate was adjusted and the experiment repeated. Cathode mass flow rates of 0.623, 0.312, and 0.125 mg/s (10, 5, and 2 SCCM) were chosen. 0.623 mg/s is the nominal cathode ignition flow rate, and 0.125 mg/s was the lowest cathode mass flow at which the cathode would stably operate.

D. Equipment

1. *Thrust Stand*

The thrust stand was a null displacement, inverted pendulum thrust stand, with automatic leveling. It was similar to the thrust stand described by Xu and Walker [16], with some differences as follows. The displacement nulling was provided by a solenoid driven by a closed-loop digital controller which measured the displacement of the thrust stand using a linear voltage displacement transducer (LVDT). The solenoid was smaller than that described by Xu and Walker, and did not require active cooling. The level is sensed by an electrolytic inclinometer, and controlled by a microstepping motor connected to an 80-threads-per-inch screw. The thrust is directly proportional to the current provided to the solenoid. As with the Xu and Walker thrust stand, calibration was provided by a linear fit to a set of known weights applied to the thruster across a pulley and controlled via a stepper motor. Typically, the calibration was performed immediately before the thruster was powered on and then again after the thruster had reached thermal equalibrium.

The data from the thrust stand and the power supplies were continually monitored by a telemetry data logger implemented in software. Communication with the thrust stand and the power supplies was either by analog input to the data logging computer, or via GPIB, depending on the device. Telemetry was recorded at a rate of 1 Hz.

From the recorded thrust, anode mass flow rate, discharge current and discharge voltage, the measured efficiency is calculated according to

$$\eta = \frac{T^2}{2\dot{m} I_d V_d} \tag{1}$$

Because we vary the cathode mass flow rate, we present both "anode efficiency," which does not include cathode mass flow:

$$\eta_a = \frac{T^2}{2\dot{m}_a I_d V_d} \tag{2}$$

and "total efficiency," which does:

$$\eta_t = \frac{T^2}{2(\dot{m}_a + \dot{m}_c) I_d V_d} \tag{3}$$

Though we have used the term "total efficiency," note that it is not quite accurate since other power sources such as the magnet and heater powers are still ignored.

2. *Hall-Effect Thruster*

The HET used in this experiment was an Aerojet BPT-2000, 2-kW class thruster [13]. The thruster has an outer diameter of ∼100 mm and a channel width of ∼10 mm. It operates at a nominal voltage of 300 V and a mass flow rate of 5 mg/s xenon. At these conditions its specific impulse is ∼1700 s with ∼50% efficiency.

3. *Cathode*

The cathode used in these experiments was a laboratory cathode similar to the MIREA cathode used by Albaréde et al. [2]. It is shown schematically in Fig. 6. The cathode consists of a 1-in.-diameter, titanium cylinder approximately 100 mm long. A 2-mm diameter orifice was drilled in one face. Pressed against this hole is a molybdenum pellet holder which holds a lanthanum-hexaboride (LaB_6) emitter. Propellant is introduced into the cathode via a feed tube attached to the side of the cylinder. Filling the length of the cathode from the pellet holder to the base is a tungsten heater coil which heats the emitter to its operating temperature. Radiation insulation loosely wraps the heater and pellet holder to maximize emitter heating. A keeper electrode is positioned approximately 3 mm outside of the orifice and is used to ignite the cathode discharge. After the main HET discharge was ignited, the keeper was unpowered and allowed to float.

In these experiments, the cathode was placed near and within the ion beam. In early trials it was found, not surprisingly, that this caused an increase in cathode temperature. While the temperature of the cathode was not directly monitored, the heater voltage was seen to increase while it was held at constant current. This is a sure indication of a temperature increase as the resistance of the tungsten filament increases with temperature, thereby causing a rise in voltage according to Ohm's law. Any heating of the cathode causes the electron emission current from the emitter to increase, which, in turn, affects the cathode coupling voltage and, therefore, the performance of the thruster. While this is interesting and may bear further research, in these experiments, we wanted to avoid this effect to isolate the effect of cathode position.

To alleviate the thermal loading of the cathode, we constructed an actively cooled shield. The shield, pictured in Fig. 6c, was a copper fin which is slightly wider than the cathode diameter and extends the length of the cathode. One-quarter-inch outer-diameter copper tubing was soldered to the base of the fin, through which water flowed during operation. The heat shield was in electrical contact with the cathode body. Teflon water supply lines were used to provide electrical isolation from ground and flexibility in cathode placement. The exposed portion of the fin was covered in graphite foil to prevent copper from contaminating the thruster or other equipment. Tests with the heat shield showed significant reduction in cathode heating. Without the shield, moving the cathode from outside the beam at 120 mm to inside the beam at 60 mm resulted in a change of 0.6 V on a nominally 10.5 V heater voltage. With the shield in place, the same change in position caused a 0.1 V change in heater voltage. Heater currents were 6 A in both cases.

4. *Mass Flow Controllers*

Flow of propellant to the thruster and the cathode was controlled by MKS Instruments Type 1479a mass flow controllers. Their accuracy was tested by monitoring the rise in pressure of a small calibration tank of known volume while flowing gas into the tank. The mass flow controllers are accurate to 1% of the full scale of the controller. The full scale for the anode controller was 200 SCCM, and it was 20 SCCM for the cathode controller. Research-grade (99.995%) krypton was used in these experiments.

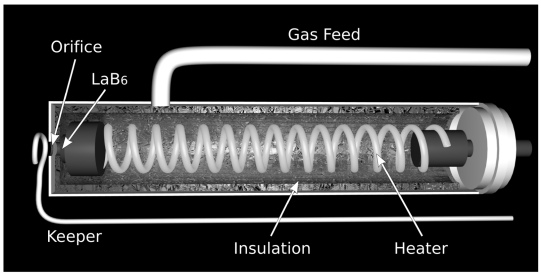

a) Schematic representation

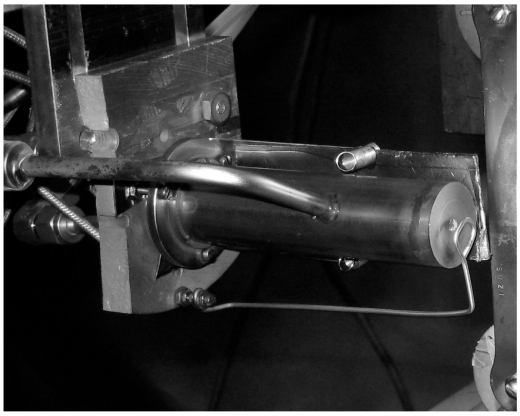

b) Photograph

c) The heat shield

Fig. 6 The laboratory cathode used in these experiments.

5. Vacuum Facility

All experiments were performed in the Xenon Vacuum Facility at Michigan Tech's Ion Space Propulsion Laboratory. The facility is a 4-m-long chamber 2 m in diameter. It is evacuated by two 48-in. cryogenic pumps capable of 60,000 L/s (nitrogen) each. The base pressure during these experiments was 5×10^{-6} Torr and operating pressures were 2.4×10^{-5} Torr as measured by an ion gauge corrected for xenon and located on the top of the downstream third of the chamber.

III. Results

A. Experiment I

The thrust, discharge current, total and anode efficiencies, and cathode coupling voltage are plotted as a function of cathode position for each pole piece and at each of the three cathode mass flow rates in Fig. 7. The r location of the separatrix at $z = 30$ mm is plotted with a dashed, vertical line for each pole piece.

Error bars are calculated estimates of the uncertainty in the measurements. The uncertainty in the thrust measurements is estimated at 2 mN based on the standard deviation of the measured thrust when operating at fixed conditions after thermal equilibrium had been reached. The uncertainty in the efficiencies are calculated according to the standard propagation of errors. For a function $f(a, b)$, the variance (the square of the uncertainty) is given by

$$\sigma_f^2 = \left(\frac{\partial f}{\partial a}\right)^2 \sigma_a^2 + \left(\frac{\partial f}{\partial b}\right)^2 \sigma_b^2 \tag{4}$$

Since the uncertainties in I_d and V_d are negligible, variance in the efficiency is given by

$$\sigma_\eta^2 = \left(\frac{T}{\dot{m}P}\right)^2 \sigma_T^2 + \left(\frac{T^2}{2\dot{m}^2 P}\right)^2 \sigma_{\dot{m}}^2 \tag{5}$$

$$= \eta^2 \left(\frac{4\sigma_T^2}{T^2} + \frac{\sigma_{\dot{m}}^2}{\dot{m}^2}\right) \tag{6}$$

Therefore, the uncertainty is given by

$$\sigma_\eta = \eta \sqrt{\frac{4\sigma_T^2}{T^2} + \frac{\sigma_{\dot{m}}^2}{\dot{m}^2}} \tag{7}$$

For anode efficiencies, we have $\dot{m} = \dot{m}_a$ and Eq. (7) may be used directly. For total efficiencies we must substitute $\dot{m} = \dot{m}_a + \dot{m}_c$. The variance of this quantity is given by

$$\sigma_{\dot{m}}^2 = \sigma_{\dot{m}_a}^2 + \sigma_{\dot{m}_c}^2 \tag{8}$$

The uncertainty in the mass flow rate is 1% of the mass flow controller's full-scale range. This yields 2 SCCM for the anode mass flow controller, and 0.2 SCCM for the cathode flow controller.

B. Experiment II

Figure 8 shows the results of the direct comparison between the EOP and OOP in Experiment II as a function of magnet current. The first and second graphs from the top show total and anode efficiencies, respectively. The third and fourth graphs show the measurements of thrust and discharge current from which the efficiencies are derived according to Eqs. (2) and (3). The bottom graph shows the cathode coupling voltages. Differing marker shapes denote the different cathode mass flow rates. Solid markers and lines denote data from the EOP, while open markers and dashed lines denote data from the OOP. With the OOP, the thruster would not operate stably at the 2 SCCM cathode flow rate, nor would it operate at any I_{mag} greater than 1.3 A when $\dot{m}_c$ was 5 SCCM.

IV. Discussion

An efficiency lower by 5%–15% was expected when running with krypton rather than xenon [17,18]. However, all of the data in this study show a 25–35% lower efficiency than when running with xenon [12]. It is not clear why such unexpectedly low efficiencies occurred, as no changes to either the thruster or the test apparatus were made between when testing using xenon and testing using krypton. The thruster was not optimized to run on krypton. It is possible that the chamber length was not sufficient to provide

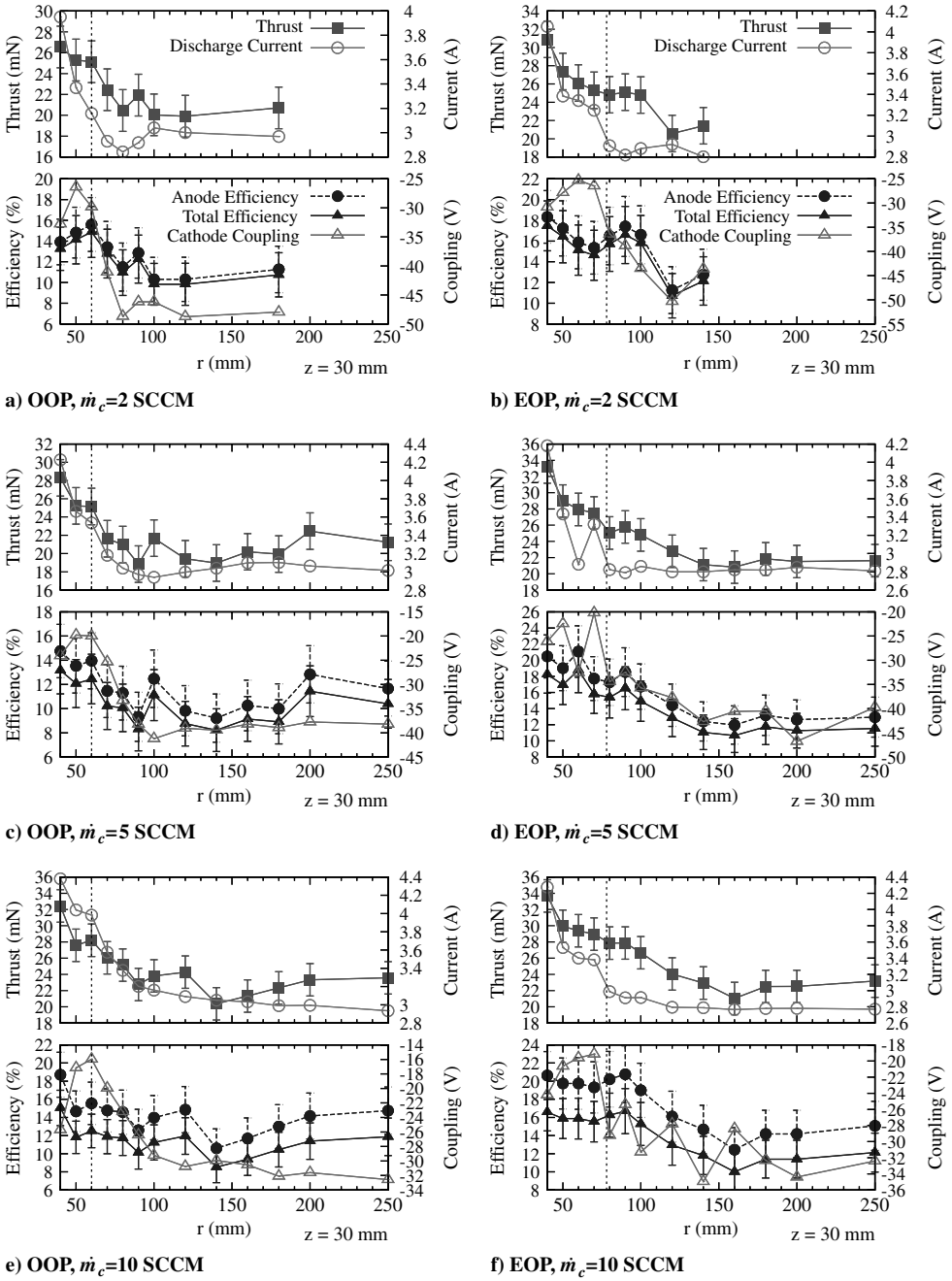

a) OOP, $\dot{m}_c$=2 SCCM **b) EOP, $\dot{m}_c$=2 SCCM**

c) OOP, $\dot{m}_c$=5 SCCM **d) EOP, $\dot{m}_c$=5 SCCM**

e) OOP, $\dot{m}_c$=10 SCCM **f) EOP, $\dot{m}_c$=10 SCCM**

Fig. 7 Thruster performance as a function of cathode position while operating on krypton.

sufficient ionization to the krypton, which has a higher ionization energy than xenon.

Several trends are apparent in the performance data shown in Fig. 7. First of all, similar trends in thrust, discharge current, efficiency and cathode coupling voltage vs cathode position are seen with the OOP data as have been seen in prior experiments [9,10,12]. The fact that these trends are similar to those seen when running xenon suggests that conclusions drawn from these data are valid, despite the change in propellant and its associated poor performance. Between 100 and 250 mm, the thrust remains relatively constant, with a slight increase as the cathode is moved out beyond 140 mm. Also in this range, the discharge current remains relatively constant, as does the cathode coupling voltage in most cases. Trends with the EOP look slightly different, with the increase in thrust occurring further out, near 160 mm. It is interesting to note that the difference in the position of the inflection point is about the same as the 18 mm difference between the separatrices of the OOP and the EOP.

Inside 100 mm, there are consistent trends of increasing thrust and discharge current and cathode position decreases. The efficiency generally increases, though in some cases it may reach a plateau inside of the separatrix. The cathode coupling voltage shows a particularly interesting trend; as r is decreased, the coupling voltage increases until the cathode crosses the separatrix, at which point it begins to decrease, though with a smaller gradient.

The increasing discharge current with decreasing r is likely due, in part, to increased ingestion of cathode propellant. The greater increases associated with cathode mass flow rates attest to this. However, the increase is too large to be totally accounted for by this effect. If we assume that the entire mass flow provided to the cathode is ingested by the anode and becomes singly ionized, then we can calculate the maximum amount of current that could be added by propellant ingestion according to:

$$\dot{N}_c = \frac{\dot{m}_c(\mathrm{SCCM}) \cdot 1 \times 10^{-6}(\mathrm{m^3/cc}) \cdot 101325\ \mathrm{Pa}}{k \cdot 273\ \mathrm{K} \cdot 60\ (\mathrm{s/\ min})} \tag{9}$$

$$I_{\mathrm{ingested}} = e\dot{N}_c \tag{10}$$

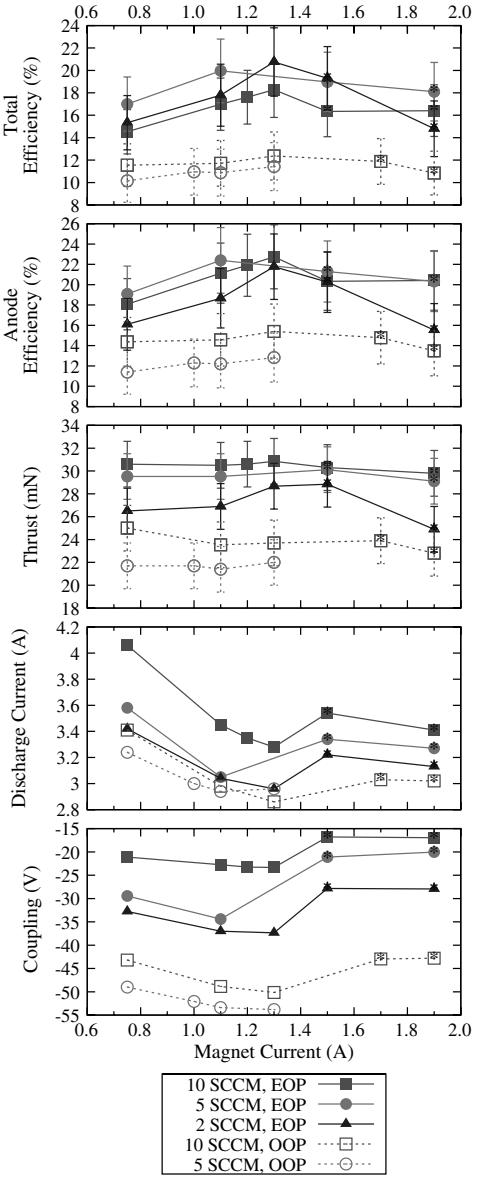

Fig. 8 Direct comparison of thruster performance when running with the OOP and EOP at identical operating conditions.

This yields a maximum possible increase in discharge current of 0.14 A, 0.36 A, and 0.72 A for $\dot{m}_c = 2$, 5, and 10 SCCM, respectively. Looking at Fig. 7, one sees that for every cathode flow rate for both the EOP and the OOP the jump in discharge current between when the cathode is placed at its farthest radial distance and at its closest is at least 1 A. Clearly, the jump in current cannot be explained by ingested propellant alone.

In most cases, particularly with the EOP, a large jump in discharge current is associated with crossing the separatrix. It is likely that by crossing the separatrix, the thruster entered a different mode of operation, which lead to increased recycle current. Despite this increase in current, the overall efficiency of the thruster was not significantly affected. The increase in thrust partially offsets the increase in discharge current in Eq. (1).

A simultaneous increase in discharge current and coupling voltage, such as that seen when the cathode is moved into the separatrix, suggests a decrease in the effective resistance between the cathode and the beam. Recall that all of the current in the beam and the recycle current to the anode originate from the cathode. A higher coupling voltage represents a smaller potential difference between the cathode and the beam. (This will be further shown in the cathode plume data discussed in Part II [14].) If the current goes up and the potential difference goes down, necessarily the resistance decreases. This suggests that moving the cathode inward, particularly across the separatrix, results in a reduction of plasma impedance between the cathode and the beam. This reduces the amount of work required to move the electrons from the cathode to the positions required to maintain charge neutrality and complete the electrical circuit. This reduced work results in increased thruster efficiency. However, as will be explored further in Part II, the change in coupling voltage is not sufficient to explain the efficiency increases seen.

It is obvious from Fig. 8 that the EOP did indeed improve the efficiency of the thruster. The figure shows that the efficiency with the EOP is five to ten percentage points greater than the efficiency with the OOP. The anode efficiency, for instance, increases from approximately 13% (on average) for the OOP to approximately 22%. Furthermore, the change is consistently outside the range of the error bars, suggesting that the change is more than the result of statistical happenstance.

The only change between the two experiments is the magnetic field topology. Therefore, it is reasonable to attribute the improved performance of the EOP to the position of the cathode in the magnetic field topology. This interpretation is further supported by the fact that the cathode coupling voltages for the OOP data are ~25 V lower than with the EOP. Defining cathode coupling efficiency as $\eta_{\mathrm{Vcg}} = (V_d + V_{\mathrm{cg}})/V_d$ yields corresponding coupling efficiencies of ~80% for the OOP compared with >90% for the EOP. Clearly the coupling is improved.

One could argue that internal rather than external magnetic field changes are responsible for the change in efficiency. As already mentioned, the simple process of placing a bigger outer pole did not control for these changes. While this is certainly possible, inspection of the internal field of the two designs, reveals small change in the internal field topology, as shown in Fig. 9. The dotted lines in parts (a) and (b) show the line sections on the exit plane and channel center extracted for quantitative comparison. The large dots indicate 0 on the line-section axis, and the arrowheads indicate the direction of positive increase. To compare the vector fields, the magnitudes along the line sections of both fields are shown in the top plots of (c) and (d). The bottom plots of (c) and (d) show the difference in field direction between the two configurations. Along the exit plane and inside the channel both magnitude and angle agree well along both cross sections except very close to the poles, where the angle difference is great. Beyond the exit plane ($z_c > 0$) the angle of the field differs more widely. In any case, a more carefully designed EOP should strive for an optimized inner field structure while modifying the external structure to move the separatrix further away from the centerline.

A second possible explanation for the improved efficiency is that the extended face may simply be directing more cathode neutrals to the discharge region, thereby making better use of the cathode propellant. This is indeed likely for more radially distant cathode positions. However, the choice of 70 mm as the cathode position for these experiments nullifies this argument as the cathode tip is nearly even with the outer edge of the outer pole with the OOP, a gap of a mere 3 mm being present. Furthermore, if the thruster were ingesting more cathode propellant with the EOP, this should be evident in an increase of discharge current in the EOP plots compared with the OOP plots of Fig. 7. If the EOP configuration was ingesting more propellant, we would expect higher discharge currents at $r=$ 70 mm, and, in fact, for every point 70 mm $\leq r \leq$ 100 mm where the cathode was in front of the face of the EOP but not the OOP. Instead, very similar discharge currents are seen across this range. Finally, we can "correct" the anode efficiency by assuming that, in the case of the EOP, all cathode propellant was ingested by the anode and singly ionized. To perform this correction, we simply take the original equation for anode efficiency [Eq. (2)] and increase the mass flow rate in the denominator appropriately

$$\eta_{a,\mathrm{corrected}} = \frac{T^2}{2\dot{m}_a I_d V_d} \frac{\dot{m}_a}{\dot{m}_a + \dot{m}_c} \tag{11}$$

which, of course, yields the same thing as the total efficiency, Eq. (3). In Fig. 8 we see that the total efficiency of the EOP thruster is higher

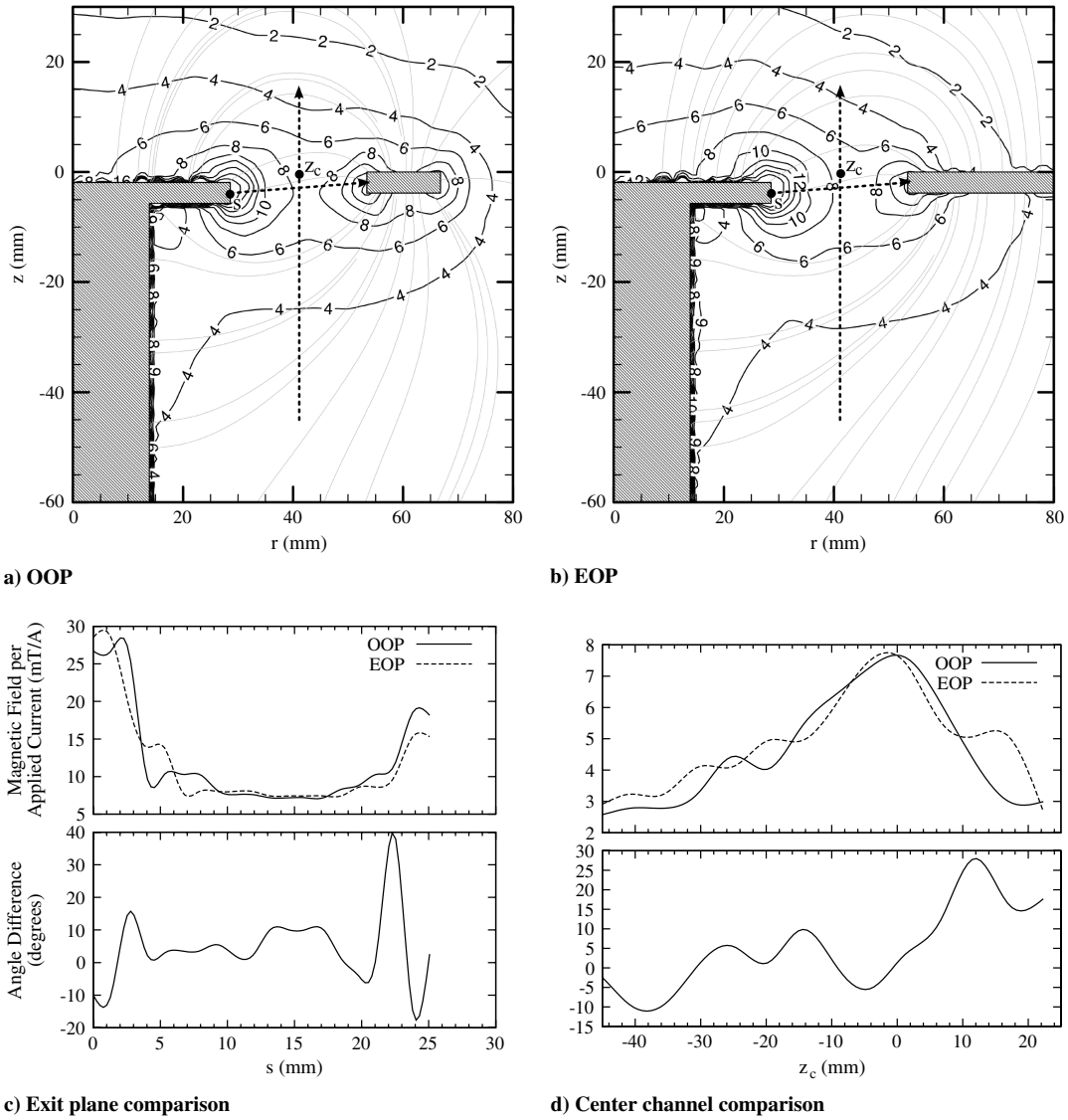

Fig. 9 Comparison of the internal magnetic fields of the thruster with the original and extended outer pole. Contours represent magnetic field strength per magnet coil current in mT/A.

than the anode efficiency of the OOP, and therefore cathode propellant ingestion cannot be the source of the improvement.[‡]

One could argue that these results should not be generalized because the thruster was not operating with its nominal propellant (xenon), and, furthermore, that it ran with poor efficiency on krypton. Given the magnitude of the change in efficiency and cathode coupling voltages seen here, however, it seems unlikely that simply using xenon would nullify these results. Nonetheless, we would not necessarily see the same 10-point improvement in efficiency for a well-tuned, OOP-type thruster operating at around 50% efficiency. The magnitude of the improvement in this case is presently unknown and is a topic for future research.

V. Conclusions

The data presented in this paper support the theory that the separatrix plays a critical role in governing cathode coupling. The data show that thrusters operated with the cathode inside of the separatrix perform significantly better than the same thruster operated with the cathode further outside the thruster. While this could be a function merely of the cathode's proximity to the discharge chamber, two facts suggest otherwise. First, minimum efficiency and cathode coupling voltages are witnessed when the cathode is near 150 mm, with an increase in both parameters as the cathode is moved further out. Second, the positions of both the minima and maxima of the cathode coupling voltage seem to move radially outward in the EOP case, where the separatrix has also moved outward as compared with the OOP case. Finally, it is clear that across a wide range of magnetic field strengths, the EOP configuration performs better than the OOP configuration with the cathode in the same location. In the case of the EOP, that location is inside the separatrix while it is outside of it for the OOP.

[‡]As an aside, it is worth pointing out that cathode propellant ingestion probably improves the total efficiency of the thruster, assuming that the ingestion does not negatively affect any of the ionization processes occurring in the thruster. As long as the cathode propellant must be expelled, better to have that propellant transformed into thrust-generating fast ions than to have it remain near the thruster as slow neutrals, or worse, back-flowing charge-exchange ions.

Acknowledgment

This work was supported by grants from the U.S. Air Force Office of Scientific Research.

References

[1] Jahn, R. G., *Physics of Electric Propulsion*, McGraw–Hill Series in Missile and Space Technology, McGraw–Hill Book Company, New York, 1968.

[2] Albarède, L., Lago, V., Lasgorceix, P., Dudeck, M., Burgova, A., and Malik, K., "Interaction of a Hollow Cathode Stream with a Hall Thruster," *28th International Electric Propulsion Conference*, IEPC Paper 03-333, March 2003.

[3] Tilley, D. L., de Grys, K. H., and Myers, R. M., "Hall thruster-cathode coupling," *35th AIAA/ASME/SAE/ASEE Joint Propulsion Conference*, AIAA Paper 99-2865, June 1999.

[4] Hofer, R. R., and Gallimore, A. D., "Recent Results From Internal and Very-Near-Field Plasma Diagnostics of a High Specific Impulse Hall Thruster," *28th International Electric Propulsion Conference*, IEPC Paper 2003-037, March 2003.

[5] Hofer, R. R., Johnson, L. K., Goebel, D. M., and Fitzgerald, D. J., "Effects of an Internally-Mounted Cathode on Hall Thruster Plume Properties," *42nd AIAA/ASME/SAE/ASEE Joint Propulsion Conference*, AIAA Paper 2006-4482, July 2006.

[6] Beal, B. E., Gallimore, A. D., and Hargus, W. A., "The Effects of Cathode Configuration on Hall Thruster Cluster Plume Properties," *41st AIAA/ASME/SAE/ASEE Joint Propulsion Conference*, AIAA Paper 2005-3678, July 2005.

[7] Walker, M. L. R., and Gallimore, A. D., "Hall Thruster Cluster Operation with a Shared Cathode," *Journal of Propulsion and Power*, Vol. 23, No. 3, May 2007, pp. 528–536. doi:10.2514/1.23688

[8] Jameson, K. K., Goebel, D. M., Hofer, R. R., and Watkins, R. M., "Cathode Coupling in Hall Thrusters," *30th International Electric Propulsion Conference*, IEPC Paper 2007-278, Sept. 2007.

[9] Sommerville, J. D, and King, L. B., "Effect of Cathode Position on Hall-Effect Thruster Performance and Cathode Coupling Voltage," *43rd AIAA/ASME/SAE/ASEE Joint Propulsion Conference*, AIAA Paper 2007-5174, July 2007.

[10] Sommerville, J. D., and King, L. B., "Effect of Cathode Position on Hall-Effect Thruster Performance and Cathode Coupling Voltage," *30th International Electric Propulsion Conference*, IEPC Paper 2007-78, Sept. 2007.

[11] Lehner, G., *Electromagnetic Field Theory for Engineers and Physicists*, Springer–Verlag, Berlin, 2010, pg. 53, Ch. 5.

[12] Sommerville, J. D., and King, L. B., "Effect of Cathode Position on Hall-Effect Thruster Performance and Near-Field Plume Peoperties," *44th AIAA/ASME/SAE/ASEE Joint Propulsion Conference and Exhibit*, AIAA Paper 2008-4996, July 2008.

[13] King, D., Tilley, D. L., Aadland, R., Nottingham, K., Smith, R., Roberts, C., Hruby, V., Pote, B., and Monheiser, J., "Development of the BPT Family of U.S. Designed Hall Current Thrusters for Commercial LEO and GEO Applications," *34th AIAA/ASME/SAE/ASEE Joint Propulsion Conference*, AIAA Paper 98-3338, July 1998.

[14] Sommerville, J. D., and King, L. B., "Hall-Effect Thruster—Cathode Coupling Part II: Ion Beam and Near-Field Plume," *Journal of Propulsion and Power*, Vol. 27, No. 4, July 2011, pp. 754–767. doi:10.2514/1.50124

[15] Sommerville, J. D., *Hall-Effect Thruster—Cathode Coupling: The Effect of Cathode Postion and Magnetic Field Topology*, Ph.D. Dissertation, Michigan Technological Univ., Houghton, MI, 2009.

[16] Xu, K., and Walker, M. L. R., "High-Power, Null-Type, Inverted Pendulum Thrust Stand," *Review of Scientific Instruments*, Vol. 80, No. 5, May 2009, p. 055103.

[17] Linnell, J. A., and Gallimore, A. D., "Efficiency Analysis of a Hall Thruster Operating with Krypton and Xenon," *Journal of Propulsion and Power*, Vol. 22, No. 6, Nov. 2006, pp. 1402–1412. doi:10.2514/1.19613

[18] Kim, V., Popov, G., Kozlov, V., Skrylnikov, A., and Grdlichko, D., "Investigation of SPT Performance and Particularities of it's Operation with Kr and Kr/Xe Mixtures," *27th International Electric Propulsion Conference*, IEPC Paper 01-065, Oct. 2001.

J. Blandino
Associate Editor